8188–8202 *Nucleic Acids Research, 2020, Vol. 48, No. 14* *Published online 16 July 2020*
doi: 10.1093/nar/gkaa602

Developing an endogenous quorum-sensing based CRISPRi circuit for autonomous and tunable dynamic regulation of multiple targets in *Streptomyces*

Jinzhong Tian [1,2], Gaohua Yang[1,2], Yang Gu [1], Xinqiang Sun[3], Yinhua Lu[4,*] and Weihong Jiang[1,*]

[1]Key Laboratory of Synthetic Biology, CAS Center for Excellence in Molecular Plant Sciences, Shanghai Institute of Plant Physiology and Ecology, Chinese Academy of Sciences (CAS), Shanghai 200032, China, [2]University of Chinese Academy of Sciences, Beijing 100039, China, [3]XinChang Pharmaceutical Factory, Zhejiang medicine LTD, Xinchang 312500, Zhejiang Province, China and [4]College of Life Sciences, Shanghai Normal University, Shanghai 200234, China

Received February 18, 2020; Revised July 01, 2020; Editorial Decision July 03, 2020; Accepted July 15, 2020

ABSTRACT

Quorum-sensing (QS) mediated dynamic regulation has emerged as an effective strategy for optimizing product titers in microbes. However, these QS-based circuits are often created on heterologous systems and require careful tuning via a tedious testing/optimization process. This hampers their application in industrial microbes. Here, we design a novel QS circuit by directly integrating an endogenous QS system with CRISPRi (named EQCi) in the industrial rapamycin-producing strain *Streptomyces rapamycinicus*. EQCi combines the advantages of both the QS system and CRISPRi to enable tunable, autonomous, and dynamic regulation of multiple targets simultaneously. Using EQCi, we separately downregulate three key nodes in essential pathways to divert metabolic flux towards rapamycin biosynthesis and significantly increase its titers. Further application of EQCi to simultaneously regulate these three key nodes with fine-tuned repression strength boosts the rapamycin titer by ∼660%, achieving the highest reported titer (1836 ± 191 mg/l). Notably, compared to static engineering strategies, which result in growth arrest and suboptimal rapamycin titers, EQCi-based regulation substantially promotes rapamycin titers without affecting cell growth, indicating that it can achieve a trade-off between essential pathways and product synthesis. Collectively, this study provides a convenient and effective strategy for strain improvement and shows potential for application in other industrial microorganisms.

INTRODUCTION

Microbes have been engineered as renewable cell factories for producing a vast array of commercially valuable products, such as pharmaceuticals, biofuels and bio-chemicals. However, most microbial cell factories are often beset with limitations such as low product titers and yields. In the past two decades, static metabolic engineering approaches, such as deleting key genes from competitive pathways or overexpressing genes from target pathways by engineering promoters or ribosome binding sites (RBS), were mainly employed to maximize product titers. However, static engineering strategies often result in metabolic imbalance, pathway intermediate accumulation and growth retardation, thus limiting product titers and yields (1,2). To address this issue, inducible promoters are one option by which strains are engineered to respond to exogenous inducers (3–5). Although this strategy is very useful for research and development purposes, it is uneconomical because of the requirement of human supervision and use of costly exogenous inducers. Recently, self-actuating, inducer-independent dynamic metabolic engineering strategies, which allow microbes to autonomously adjust the metabolic networks in response to environmental changes in real-time, have been developed and applied to efficiently optimize microbial cell factories (6–11).

These dynamic control systems are mainly implemented in two different manners: pathway-dependent and pathway-independent regulation. Pathway-dependent control systems are generally employed to redirect metabolic fluxes in response to changes in the concentrations of pathway intermediates or byproducts. Characterization of a pathway-specific biosensor, such as a metabolite-responsive transcription factor or riboswitch, is necessary to achieve dynamic regulation (7,12). This strategy has been used to sig-

*To whom correspondence should be addressed. Tel: +86 21 64322208; Fax: +86 21 64322762; Email: yhlu@shnu.edu.cn
Correspondence may also be addressed to Weihong Jiang. Tel: +86 21 54924172; Fax: +86 21 54924015; Email: whjiang@sibs.ac.cn

nificantly improve the production of a number of value-added products in various microbes, such as lycopene (13), fatty acid ethyl ester (14), amorphadiene in *Escherichia coli* (15), lysine in *Corynebacterium glutamicum* (16) and *N*-acetylglucosamine in *Bacillus subtilis* (17). Pathway-independent dynamic control, which utilizes common regulatory elements, such as quorum-sensing (QS) circuitry, to couple gene expression to the physiological state of the cell, has also been applied to improve product titers and yields (18–22). QS systems function to control cell density-dependent processes, which are ubiquitous in microbes, such as the LasI/LasR and RhlI/RhlR systems in *Pseudomonas aeruginosa* (23), LuxI/LuxR in *Vibrio fischeri* (24), EsaI/EsaR in *Pantoea stewartii* (25), and the γ-butyrolactones (GBLs) signaling systems in streptomycetes (26). Typically, each QS system is composed of a synthase (e.g. LuxI) responsible for synthesizing specific small-molecule signals (e.g. acyl-homoserine lactone), and a cognate signal-responsive transcription regulator (e.g. LuxR). Accumulation of signals (at a high cell density) results in activation or deactivation of target genes. Placing the gene of interest under the control of signal-responsive regulators can achieve cell density-dependent gene regulation. QS-mediated dynamic regulation has broader applicability and can be implemented across different pathways without developing a specific biosensor. However, in bacteria, all pathway-independent QS circuits are built on heterologous systems, such as the *lux* system from *V. fischeri* (20,22) and the *esa* system from *P. stewartii* (19–21). For these circuits to function effectively, appropriate switching times and desired regulation strength in hosts must be achieved by repeated testing, screening, and optimization of *cis*-regulatory elements (promoter and RBS) that drive the expression of QS circuits. This prevents their wider application in industrial microbes. To address these challenges, we aimed to develop a pathway-independent dynamic control circuit by directly harnessing endogenous QS elements (e.g. QS-responsive promoters). Additionally, to enable efficient regulation of multiple pathways simultaneously, we attempted to integrate the *e*ndogenous *Q*S element with the gene repression *C*RISPRi tool (named as EQCi) for pathway-independent regulation. CRISPRi, which was developed based on the DNase-inactivated CRISPR/Cas endonucleases, such as dCas9 (27,28), has emerged as an effective tool using which the expression of multiple target genes can be fine-tuned (29,30). Importantly, the gene repression strength can be optimized by adjusting the expression of dCas9 and single guide RNA (sgRNA), or by simply changing the targeting position of the sgRNA (28,31).

Streptomyces is an important industrial microbe that is regarded as a rich reservoir of antibiotics and other valuable natural products, which are widely used in medicine, agriculture, and animal husbandry. However, in most cases, industrial scale-up production of natural products using *Streptomyces* is limited by low titers. As the biosynthesis of natural products involves competition for common precursors with primary pathways (particularly central carbon metabolism), which are essential for cell growth and cannot be deleted from the genome, we attempted to apply the EQCi strategy to boost natural product titers by dynamically knocking down key nodes in essential pathways. Rapamycin, produced by *Streptomyces rapamycinicus*, was selected as an example to validate our EQCi system. This natural product exhibits a broad range of biological activities, including immunosuppressive, antitumor and neuroprotective/neuroregenerative activities (32). It has been approved as an immunosuppressant and its derivatives have been approved as antitumor drugs. Recent studies showed that rapamycin has anti-aging activities, including a significant extension of the life spans of yeast, fruit flies, nematodes and mice (32), in addition to slowing down the aging of human skin (33). However, the industrial rapamycin-producing *S. rapamycinicus* must be further optimized to develop an economically viable process.

To this end, we constructed an EQCi system in *S. rapamycinicus*, in which the *dcas9* gene was regulated by a native QS signal-responsive promoter and sgRNA by a synthetic strong promoter *j23119* from *E. coli* (http://parts.igem.org/). The design of EQCi, which integrates the endogenous QS element and CRISPRi, enabled us to implement dynamic downregulation of multiple essential pathway genes to redirect metabolic flux toward rapamycin biosynthesis in a cell density-dependent manner. EQCi-mediated regulation was applied to downregulate three respective key nodes in the TCA cycle, the fatty acid (FA) synthesis pathway and the aromatic amino acid (AAA) synthesis pathway, resulting in significantly enhanced rapamycin titers. We further applied EQCi to downregulate three key nodes simultaneously and achieved the highest reported titer by screening of a library of sgRNA combinations with varying repression strengths. The data clearly demonstrated that EQCi-based regulation is a convenient and effective strategy that balances multiple essential pathways to promote product titers, and that it can be broadly applied to other industrial microorganisms.

MATERIALS AND METHODS

Bacterial strains, plasmids and growth conditions

Plasmids and bacterial strains used in this study are listed in Supplementary Table S1. *E. coli* strains, including DH5α and ET12567/pUZ8002, were grown at 37°C in Luria-Bertani (LB) broth or on LB agar plates. DH5α was used for general cloning and ET12567/pUZ8002 was employed as the donor strain for intergenic conjugation between *E. coli* and *Streptomyces*. *S. rapamycinicus* 2001 was derived from the wild-type strain NRRL 5491 by recursive physical and chemical mutagenesis, and grown at 30°C on oat agar medium (20 g/l oat, 20 g/l agar, pH 6.8) for preparing spore suspensions and on M-ISP4 (2 g/l tryptone, 1 g/l yeast extract, 5 g/l soya flour, 5 g/l mannitol, 5 g/l starch, 2 g/l calcium carbonate, 1 g/l sodium chloride, 0.5 g/l valine, 20 g/l agar) for intergenic conjugation. *Streptomyces coelicolor* M145 was grown on MS medium (20 g/l soybean flour, 20 g/l mannitol, 20 g/l agar) for spore preparation as well as intergenic conjugation. When necessary, apramycin (50 μg/ml), kanamycin (50 μg/ml) and nalidixic acid (25 μg/ml) were added.

β-Galactosidase reporter assays

The codon optimized thermophilic *lacZ* gene (34) under the control of the GBL-responsive promoter *srbAp* or the strong constitutive promoter *ermEp** (GenScript, Nanjing, China) was cloned in the integrative vector pSET152 between NdeI and XbaI to yield the plasmids, pSET-*srbAp-lacZ* and pSET-*ermEp*-lacZ*. The two plasmids were individually transferred into *S. rapamycinicus* 2001 by intergenic conjugation. Strains harboring the reporter plasmids were plated on oat agar medium and cultured at 30°C for 7 days. Strain 2001 with the empty plasmid pSET152 (2001-p) was used as a control. Agar cultures were inoculated into 25 ml of seed medium (15 g/l soluble starch, 3 g/l peptone, 0.5 g/l L-lysine, 1.0 g/l $K_2HPO_4{\cdot}3H_2O$, 3 g/l glucose, pH 7.0) in 250 ml flasks at 28°C for 24 h. Then, 3 ml of seed cultures were transferred into 25 ml of fermentation medium (4 g/l soybean flour, 2 g/l peptone, 10 g/l oat, 5 g/l glycerol, 1.5 g/l L-lysine, 40 g/l glucose, pH 6.5) in 250 ml flasks at 28°C. Cultures were collected every 12 h (12-192 h) by centrifugation at 12 000g for 5 min. Cell pellets were dissolved in the B-PER reagent (Thermo Scientific Pierce, USA) and vortexed for 1 min. The resulting cell lysates were heated at 60°C for 30 min to remove heat unstable proteins (such as endogenous β-galactosidases), followed by centrifugation for 30 min at 12 000g. The supernatants were used for the β-galactosidase assays as previously reported (34). The experiments were performed with three biological replicates.

Construction of the CRISPRi plasmids and the corresponding engineered strains

The *ermEp**-driving CRISPRi plasmids were constructed based on pSET-*dcas9-actII4-NT-S1* by simply replacing the 20-nt specific guide sequence (N20) of sgRNA targeting the non-template (NT) strand of genes of interest according to the method described previously (35). N20 guide sequences of sgRNA were designed by the online software CRISPy (http://crispy.secondarymetabolites.org/) (36). Here, the construction process of pSET-*ermEp*-dcas9/sg-fabH3* was described as an example. Briefly, the sgRNA (*sg-fabH3*) expression cassette harboring the sequences of the *j23119* promoter, *sg-fabH3* and T0 terminator was amplified by PCR using the primer pair sg-fabH3-F/sgRNA-R and the plasmid pSET-*dcas9-actII4-NT-S1* was used as the template. The obtained PCR product was digested by SpeI and EcoRI, and cloned into pSET-*dcas9-actII4-NT-S1* digested with the same two restriction enzymes, resulting in pSET-*ermEp*-dcas9/sg-fabH3*.

The control CRISPRi plasmid, pSET-*ermEp*-dcas9*, harboring the sgRNA scaffold without N20 sequence was similarly constructed, based on pSET-*dcas9* (36). The control EQCi plasmids, namely, pSET-*srbAp-dcas9* (for *S. rapamycinicus*) and pSET-*scbAp-dcas9* (for *S. coelicolor*) harboring the sgRNA scaffold without N20 sequence, were generated based on pSET-*ermEp*-dcas9* by replacing *ermEp** with the *srbAp* and *scbAp* promoters, respectively. Briefly, the *srbAp* and *scbAp* promoters were individually amplified from the genomes of *S. rapamycinicus* 2001 and *S. coelicolor* M145 by PCR using the primer pair *srbAp*-F/R and *scbAp*-F/R. Two PCR products were digested with XbaI and NdeI and cloned into pSET-*ermEp*-dcas9*, which was treated with the same two enzymes, thus generating pSET-*srbAp-dcas9* and pSET-*scbAp-dcas9*.

The EQCi plasmids pSET-*srbAp-dcas9-sgRNA* or pSET-*scbAp-dcas9-sgRNA* for dynamic regulation of single genes were generated based on pSET-*srbAp-dcas9* or pSET-*scbAp-dcas9* by simply inserting the 20-nt guide sequence (N20) of a specific sgRNA as the process for the construction of pSET-*ermEp*-dcas9/sg-fabH3*.

A library of 18 EQCi plasmids harboring different combinations of three sgRNAs (targeting *fabH3*, *gltA2* and *cm2*) for multiplex gene repression were constructed by GenScript (Nanjing, China). The DNA sequences of 18 different sgRNA combinations were presented in the Supplementary Data.

The plasmids pSET-*srbAp-dcas9*–3 × Flag and pSET-*ermEp*-dcas9*-3× Flag with the 3× Flag tag sequence inserted before the stop codon of the *dcas9* gene was constructed from pSET-*srbAp-dcas9* and pSET-*ermEp*-dcas9*, respectively, using a homologous recombination technology. Briefly, the 3× Flag tag sequence was amplified by overlapping PCR using the primer pair *dcas9*-3× Flag-F/R. The obtained PCR product was cloned into pSET-*srbAp-dcas9* and pSET-*ermEp*-dcas9* digested with SwaI, respectively, by the One-step Cloning Kit CloneExpress® MultiS (Vazyme, China), generating the plasmids pSET-*srbAp-dcas9*-3× Flag and pSET-*ermEp*-dcas9*-3× Flag.

The correctness of all the constructed plasmids were confirmed by DNA sequencing. Then, the CRISPRi plasmids were individually introduced into the parental strain 2001, generating the engineered strains harboring the corresponding CRISPRi plasmid. The primers are listed in Supplementary Table S2.

Construction of the strains 2001/*srbA*-3× Flag and 2001/*srbR*-3× Flag

The engineered *S. rapamycinicus* strains of 2001/*srbA*-3× Flag and 2001/*srbR*-3× Flag with the 3× Flag tag sequence inserted before the stop codons of *srbA* and *srbR*, respectively, were constructed based on the parental strain 2001 by the traditional homologous recombination-mediated method (37). Here, the construction process of 2001/*srbA*-3× Flag was described as an example. Briefly, the upstream (1525 bp) and downstream (1811 bp) homologous arms (harboring the 3× Flag tag sequence) were amplified from the *S. rapamyinicus* genome by PCR using the primer pairs of *srbA*-3× Flag-Up-F/R and *srbA*-3× Flag-down-F/R, respectively. Two obtained PCR products were ligated together by overlapping PCR using the primers of *srbA*-3× Flag-Up-F/down-R. The resultant DNA fragment *srbA*-up-3× Flag-down was cloned into the replication temperature-sensitive plasmid pKC1139 (digested with HindIII and EcoRI) by the One-step Cloning Kit CloneExpress® MultiS (Vazyme, China), resulting in pKC-*srbA*-up-3× Flag-down. The obtained plasmid was introduced into *S. rapamycinicus* by conjugal transfer. The mutants with the 3× Flag tag sequence inserted into the *srbA* gene by screening for single crossovers and double crossovers, respectively. The correct mutants were checked by colony PCR, followed by DNA sequencing. The mutant was named as 2001/*srbA*-3× Flag. Similarly, the plasmid

pKC-*srbR*-up-3× Flag-down and the mutant 2001/*srbR*-3× Flag were constructed. The primers are listed in Supplementary Table S2.

S. rapamycinicus fermentation and HPLC analysis of rapamycin production

Spores of *S. rapamycinicus* strains were streaked on oat agar medium and cultured at 30°C for 7 days. Agar cultures were inoculated into 25 ml of seed medium in 250 ml flasks at 28°C for 24 h. Then, 3 ml of seed cultures were transferred into 25 ml of fermentation medium in 250 ml flasks. 0.5 ml of fermentation cultures were extracted with equal volume of methanol at room temperature for 1 h. After centrifugation at 12 000 rpm for 10 min, supernatants were analyzed by HPLC using a reversed-phase column (Shimadzu, shim-pack VP-ODS, 4.6 um, 4.6 × 150 mm). A mixture of water/methanol (15:85) was used as the mobile phase, with a flow rate of 1.0 ml/min and a retention time of 12 min. Rapamycin was monitored at a wavelength of 277.4 nm. The experiments were carried out with three biological replicates.

Quantitative analysis of actinorhodin production

100 μl spores of pre-germinated *S. coelicolor* strains (OD_{450} was adjusted to 0.8) were evenly coated on YM agar medium (oat powder 20 g/l, agar 20 g/l, pH 6.8) covered with cellophane, and grown at 30°C. Samples were collected at five time points (24, 48, 72, 96 and 120 h) and dried at 70°C for 8 h, and weighed. KOH was added at a final concentration of 1 M. After incubation at room temperature for 1 h, samples were centrifuged at 12 000 g for 5 min. The absorbance of the supernatants was assayed at the wavelength of 640 nm. The actinorhodin titers were indicated as optical density at 640 nm (OD_{640})/g (dry weight). The experiments were conducted with three biological replicates.

Determination of *S. rapamycinicus* growth curve

The biomass of *S. rapamycinicus* strains was measured by a simplified diphenylamine colorimetric method as described before (38). In brief, *S. rapamycinicus* strains were grown on oat agar medium at 30°C for 7 days. Agar cultures were inoculated into 25 ml of seed medium in 250 ml flasks at 28°C for 24 h. Subsequently, 3 ml of seed cultures were transferred into 25 ml of fermentation medium in 250 ml flasks at 28°C. Samples (0.5 ml) were collected at an interval of 12 h, followed by centrifugation at 12 000 g for 5 min. Cell pellets were dissolved in the diphenylamine reaction buffer (diphenylamine 1.5 g, glacial acetic acid 100 ml, concentrated sulfuric acid 1.5 ml, 1.6% aqueous acetaldehyde 1 ml) and vortexed for 1 min. The reactions were incubated for 1 h at 60°C, followed by centrifugation for 1 min at 12 000 g. OD_{595} of the supernatants were assayed by the multifunctional microtiter plate reader Tecan Spark (Tecan, Switzerland). The experiments were performed with three biological replicates.

Quantification of mRNA

Real-time RT-PCR (RT-qPCR) analysis was conducted as reported previously (39). Briefly, cultures were taken at four time points (3, 5, 7 and 9 days) and frozen quickly in liquid nitrogen and then ground into powder. RNA samples were extracted with the Ultrapure RNA Kit (SparkJade, Shanghai, China) and followed by digestion with DNase I (SparkJade, Shanghai, China) to remove residual chromosomal DNA. RT-qPCR was carried out in a MyiQ2 thermal cycler (Bio-Rad, USA), using a SYBR Green PCR premix kit (Bio-Rad, USA). PCR analysis was carried out in triplicate (technical replicates). The relative transcript levels of each tested gene were normalized to *hrdB* (*M271_14880*, an internal control) and the relative fold changes of gene transcription (the tested strains versus the control strains) were then determined by the $2^{-\Delta\Delta CT}$ method (40). The values are averages of three independent RT-qPCR analysis. The experiments were conducted with three independent RNA samples (biological replicates). Error bars indicate the standard deviations (SD). The primers used are listed in Supplementary Table S2.

Western-blot analysis

S. rapamycinicus strains were grown in fermentation medium and 3 ml of the cultures were collected at four time points (3, 5, 7 and 9 days). After centrifugation at 5000 g, cell pellets were suspended in 7 ml of the protein purification buffer (50 mM Tris–HCl, 0.5 mM EDTA, 50 mM NaCl, 5% glycerol, pH 7.9) and lysed by sonication using the sonicator, JY92-IIN (SCIENTZ, china). The protein concentrations of whole cell lysates were determined using a BCA Protein Assay Kit (Sangon, China). The same amount of protein samples (20 μg) from different *S. rapamycinicus* strains was separated by 12% SDS-PAGE and then transferred to PVDF membranes for 45–60 min at 400 mA. The membranes were blocked at room temperature in 1× TBST buffer (10 mM Tris–HCl, 100 mM NaCl and 0.2% Tween-20, pH 7.4) containing 5% nonfat dry milk. After incubation for 30 min, the anti-3× Flag antibody (ABclonal, China) was added at a dilution rate of 1:15 000 (v/v) and incubated for 1 h, followed by washing with TBST three times. Then, goat horseradish peroxidase-conjugated anti-mouse antibody (ABclonal, China) diluted in TBST (1:5000) was used as the secondary antibody and incubated with the membrane for 1 h, followed by washing with TBST three times. Finally, the ECL substrate was added to the membrane and signals were detected by the ImageQuant LAS 4000 mini (GE, USA) according to the instructions provided by the manufacturer.

RESULTS

Design of an endogenous QS system-based CRISPRi circuit (EQCi) for autonomous and dynamic gene regulation in *S. rapamycinicus*

In *Streptomyces*, the QS system is critical for coordinating the initiation of natural product biosynthesis, which is achieved by GBLs and their cognate receptors (TetR family regulators) (26). During exponential growth phase (at a low cell density), the cytoplasmic receptors bind to their target DNA sites in the promoter regions and repress gene transcription. Upon sensing a certain concentration of GBLs (at a high cell density, normally transi-

tion phase), GBLs bind to the receptors and inhibit their DNA-binding activity, resulting in transcription derepression. QS systems have been intensively investigated in several streptomycetes, such as AfsA/ArpA from *Streptomyces griseus* (41), ScbA/ScbR from *Streptomyces coelicolor* (42,43) and SbbA/SbbR from *Streptomyces bingchengensis* (44). Among them, AfsA, ScbA, and SbbA are proteins involved in GBL biosynthesis, whereas ArpA, ScbR, and SbbR function as the GBL receptors. Notably, the biosynthesis of GBLs is not well-understood. In addition to AfsA, ScbA and SbbA, other proteins may also be involved. Recently, in *S. coelicolor*, two enzymes, namely, ScbB and ScbC, which encode a 3-ketoacyl-ACP/CoA reductase and a butanolide phosphate reductase, respectively, were found to be involved in the biosynthesis of three GBLs, SCB1 to SCB3 (45).

BLASTp analysis revealed the potential presence of a QS system encoded by *M271_07485* and *M271_07490*, referred to as SrbA and SrbR, in *S. rapamycinicus*. They displayed a high amino acid sequence identity with the GBL synthesis proteins and receptors from *S. coelicolor* (ScbA/ScbR) and *S. bingchengensis* (SbbA/SbbR) (Supplementary Figure S1A). Furthermore, the promoter region of *srbA* showed high DNA sequence identity with that of *sbbA* from *S. bingchengensis* (Supplementary Figure S1B), the transcription of which is directly regulated by SbbR (44). This clearly suggests that the promoter region of *srbA* (*srbA*p) is regulated by SrbR and that *srbA*p acts as a GBL-responsive promoter in *S. rapamycinicus*.

To characterize the activity of *srbA*p, *srbA*p-driving expression of a thermophilic *lacZ* (34) cloned on an integrative plasmid, pSET152, was constructed, resulting in the plasmid pSET-*srbA*p-*lacZ*. A recombinant plasmid pSET-*ermEp**-*lacZ*, in which the most widely used constitutive promoter in *Streptomyces*, *ermEp**, was used to drive *lacZ* expression, was also constructed as a control (Figure 1A). In *S. rapamycinicus*, very few promoters were well-characterized and gene overexpression was always driven by *ermEp**. Therefore, in this study, this promoter was used as an example of the static metabolic engineering strategy. These two plasmids were individually introduced into *S. rapamycinicus* 2001. As an empty control, 2001 with pSET152 (2001-p) was also constructed. No difference in bacterial growth was observed upon LacZ expression compared to the parental strain 2001 and 2001-p (Figure 1B). Continuous measurements of β-galactosidase activity revealed that the strain with pSET-*ermEp**-*lacZ* (2001/*ermEp**-*lacZ*) showed very high enzyme activity even at low cell population densities, which was due to constitutive expression of *ermEp**. However, the strain harboring pSET-*srbAp-lacZ* (2001/*srbAp-lacZ*) showed high enzyme activity only when the cell density reached a high level (Figure 1B). This result is consistent with our understanding of the working model of the QS system in *Streptomyces*, clearly indicating that *srbAp* was a GBL-responsive promoter.

The EQCi circuit was designed in a manner via which *srbA*p was used to drive dCas9 expression and the well-characterized synthetic promoter *j23119* was used to regulate the transcription of sgRNAs targeting the genes of interest (Figure 1C). At a low cell population density of *S. rapamycinicus* (indicating that the GBL concentration was low), the GBL receptor SrbR bound to *srbAp*, resulting in the repression of dCas9 expression and switching off of the EQCi circuit. When the cell density was high and the GBL concentration reached a threshold level, GBL binding resulted in the release of SrbR from *srbAp*, thereby leading to dCas9 expression, which switched the EQCi circuit on. The cell density-dependent, dynamic behavior of the EQCi system was confirmed by monitoring the protein levels of the QS elements (SrbA and SrbR) and dCas9 (Supplementary Figure S2). Considering that the GBL chemical structure in *S. rapamycinicus* has not been determined, the GBL concentrations were not monitored to further understand the dynamic behavior of the EQCi system. However, the behavior of the EQCi circuit may enable dynamic repression of the expression of any gene of interest or a combination of multiple genes in a cell density-dependent manner and can be used to favor accumulating rapamycin by rebalancing the metabolic flux distribution between bacterial growth and rapamycin biosynthesis. Here, key nodes from three essential pathways (TCA cycle, FA synthesis pathway, and AAA synthesis pathway; Figure 1D), were selected to be dynamically downregulated by EQCi circuits to divert carbon flux away from primary metabolism towards rapamycin biosynthesis, thereby boosting rapamycin titers in *S. rapamycinicus*. For comparison, *ermEp**-driving CRISPRi circuits for static downregulation, in which *ermEp** was used to drive dCas9 expression, were constructed in some cases (Figure 1C). Constitutive dCas9 expression was verified in the strain 2001/*ermEp**-*dcas9*-3× Flag (2001 with the control *ermEp**-driving CRISPRi plasmid, pSET-*ermEp**-*dcas9*-3× Flag) by western-blot analysis (Supplementary Figure S2).

EQCi-mediated dynamic control of the FA synthesis pathway

The biosynthesis of each rapamycin molecule requires seven malonyl-CoA extension units (32). Low endogenous malonyl-CoA levels always act as a limiting factor in rapamycin biosynthesis. Here, as a proof of concept, we applied EQCi genetic circuits to elevate malonyl-CoA by dynamically downregulating the FA synthesis pathway. As the 3-oxoacyl-ACP synthase is a key enzyme that regulates the entry of acetyl-CoA and malonyl-CoA into the FA synthesis pathway, genes encoding this key node were selected for dynamic regulation. In *S. rapamycinicus*, three genes, namely, *fabH1 (M271_17610)*, *fabH2 (M271_33380)* and *fabH3 (M271_41260)*, were predicted to be responsible for this key node (KEGG, https://www.kegg.jp/). For each gene, one sgRNA was designed to target the nucleotide (nt) positions of nt 27–46 (*fabH1*) (*sg-fabH1*), nt 8–27 (*fabH2*) (*sg-fabH2*) and nt 179–198 (*fabH3*) (*sg-fabH3*) with respect to the start codons. Accordingly, three EQCi plasmids (pSET-*srbAp-dcas9*/*sg-fabH1*, pSET-*srbAp-dcas9*/*sg-fabH2* and pSET-*srbAp-dcas9*/*sg-fabH3*) were constructed (Supplementary Table S1). As controls, three *ermEp**-driving CRISPRi circuits for static downregulation, namely, pSET-*ermEp**-*dcas9*/*sg-fabH1*, pSET-*ermEp**-*dcas9*/*sg-fabH2* and pSET-*ermEp**-*dcas9*/*sg-fabH3* were also constructed (Supplementary Table S1). Six CRISPRi plasmids were introduced into *S. rapamycinicus* 2001, respectively. Analysis

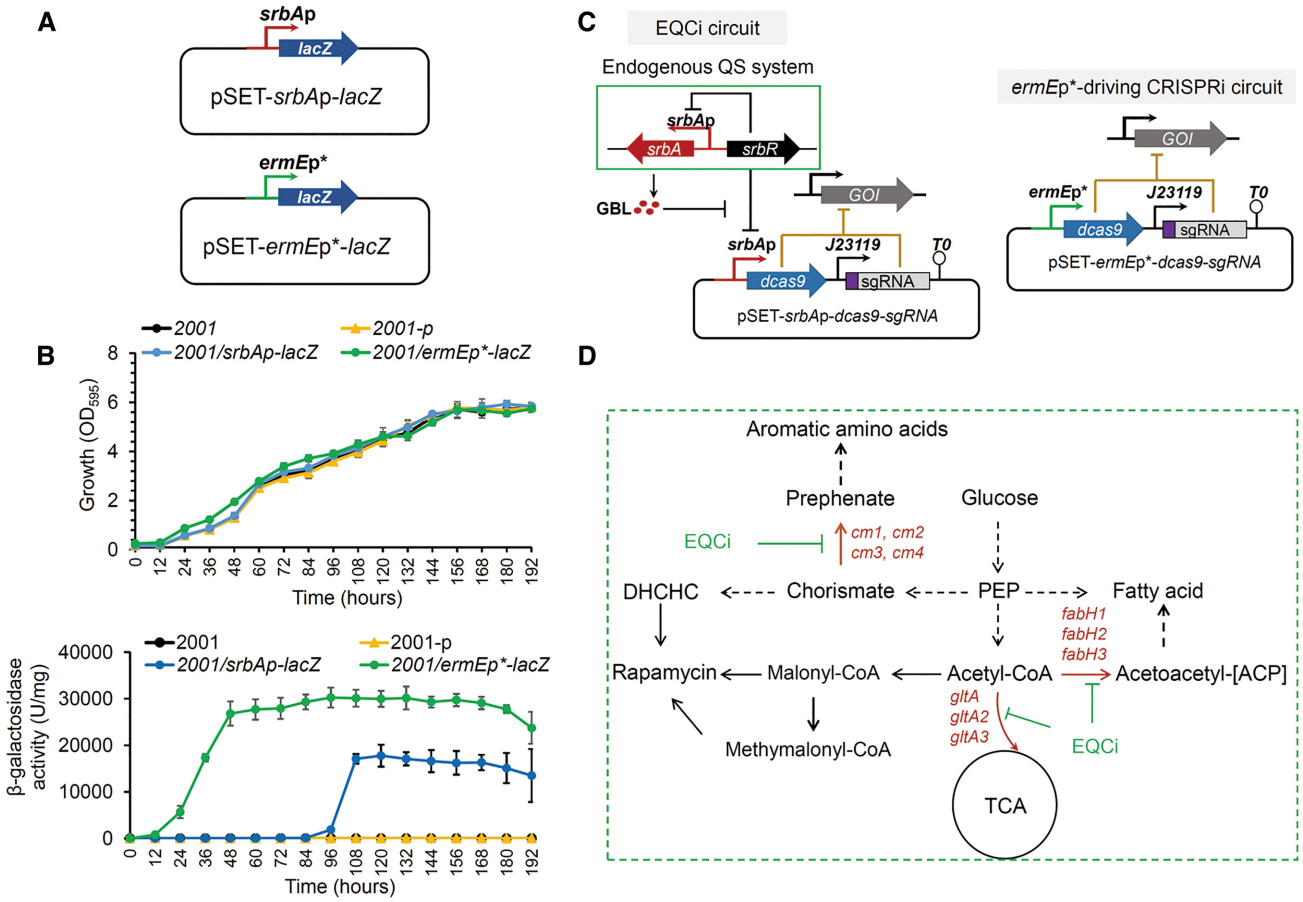

Figure 1. Characterization of the *srbAp* promoter and design of the EQCi genetic circuit in *S. rapamycinicus.* (**A**) Schematic diagram of two reporter systems in which the *lacZ* gene was regulated by the constitutive strong promoter *ermEp** and the GBL-responsive promoter *srbAp*, respectively. The integrative plasmid pSET152 was used as the backbone for the construction of reporter systems. (**B**) β-galactosidase activities normalized to the biomass of *S. rapamycinicus* harboring the reporter plasmid pSET-*ermEp*-lacZ* or pSET-*srbAp-lacZ*. The parental strain 2001 and 2001 harboring pSET152 (2001-p) were used as controls. Error bars represent the standard deviations (SD) of three biological replicates. (**C**) Architecture of the EQCi-based genetic circuit. pSET152 was used as the backbone for the construction of EQCi genetic circuits, in which *srbA*p was used to drive dCas9 expression and the synthetic strong promoter *j23119* from *E. coli* was used to drive the transcription of sgRNA targeting the gene of interest (GOI). The *ermEp**-driving CRISPRi circuit for static regulation was used as a negative control, in which *ermEp** was used to drive dCas9 expression and *j23119* was used to regulate sgRNA transcription. (**D**) Schematic diagram of some essential metabolic pathways in *S. rapamycinicus*. Three key nodes selected as the targets of EQCi-mediated downregulation are shown by red color. Each node involves three or four genes as indicated. EQCi-mediated dynamic repression will divert metabolic flux from essential pathways to rapamycin biosynthesis in a cell density-dependent manner.

of rapamycin production revealed that the EQCi circuit-mediated dynamic repression of *fabH1*, *fabH2* and *fabH3* all resulted in significantly elevated rapamycin production. The maximal titer was achieved by dynamic repression of *fabH3*, which reached 808 ± 21 mg/l; this value was ∼230% higher than those of two control strains, 2001/*srbAp-dcas9* (2001 with the control EQCi plasmid, pSET-*srbAp-dcas9*) and 2001 (Figure 2A). However, these three strains containing the *ermEp**-driving CRISPRi circuits produced drastically lower rapamycin titers than those of the controls (Figure 2B). Growth curve analysis revealed that strains carrying the EQCi circuit for downregulation of *fabH1* and *fabH2* accumulated slightly lower biomass than those of 2001 and 2001/*srbAp-dcas9*, whereas the strain for dynamic regulation of *fabH3* grew similarly well compared to the controls (Figure 2C). However, the three strains with static regulation circuits showed drastically impaired bacterial growth compared to the two control strains (Figure 2D).

To further characterize the behavior of the EQCi circuits, we analyzed the transcript levels of *fabH1*, *fabH2* and *fabH3* in strains with either the EQCi or *ermEp**-driving CRISPRi circuits. The transcript levels of *fabH1*, *fabH2*, and *fabH3* in strains with *ermEp**-driving CRISPRi circuits were drastically downregulated to 6.7–14%, 3.3–8.2% and 7.2–12.4%, respectively, of the control strain 2001/*ermEp*-dcas9* throughout the tested time course of 3, 5, 7 and 9 days (Figure 2F). Although EQCi circuits had little effect on the transcription of *fabH1*, *fabH2* and *fabH3* during the early growth stage (3 days), a significant decrease in gene transcription was detected starting on day 5 (Figure 2E), clearly indicating that gene repression occurred in a cell density-dependent manner. As controls, individual introduction of the plasmids (pSET-*srbAp-dcas9* and pSET-*ermEp*-dcas9*) into 2001 had little effect on the transcription of *fabH1-H3* (Supplementary Figure S3). The transcription data clearly suggested that static, constitutive downregulation of a key

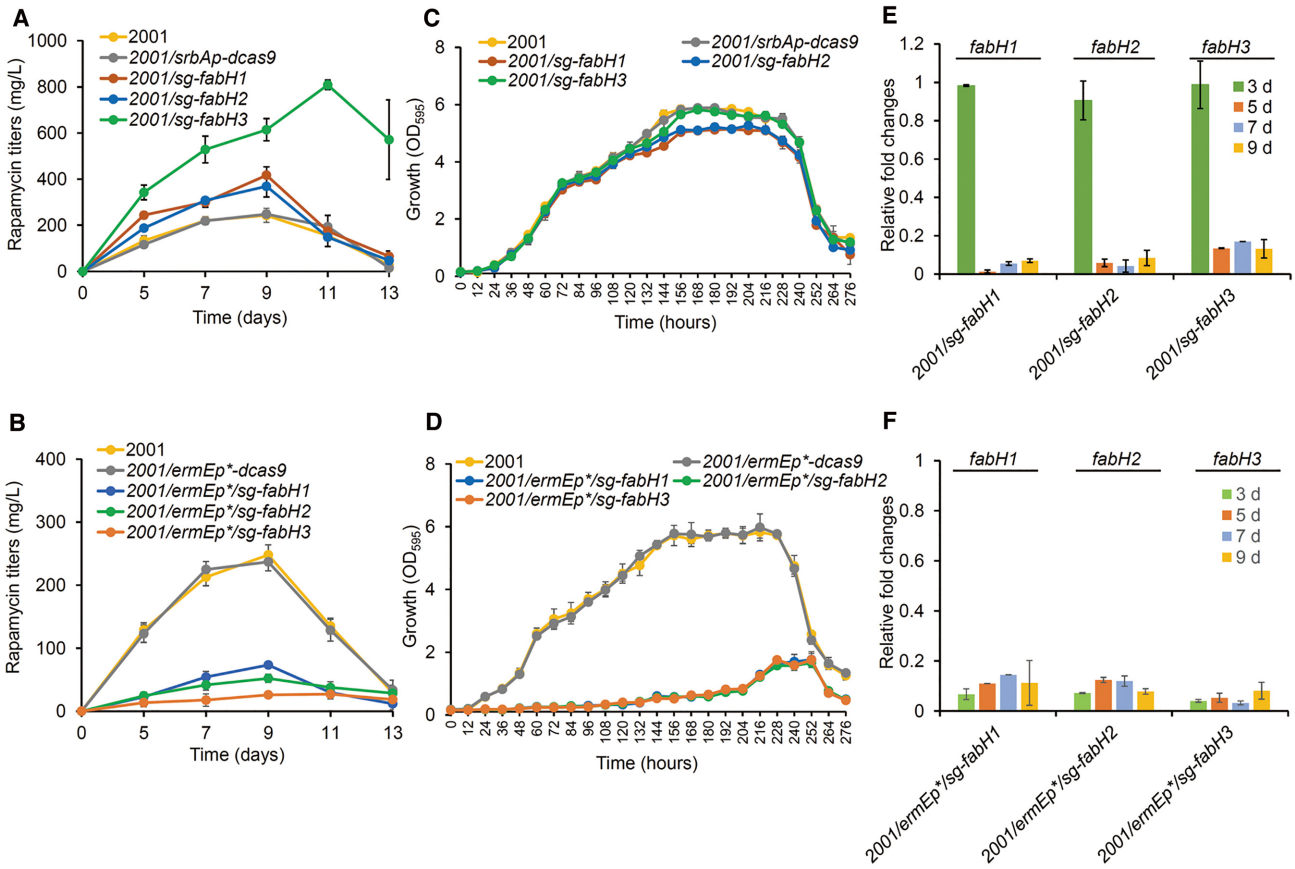

Figure 2. Effects of EQCi-mediated dynamic repression of the key node (3-oxoacyl-ACP synthase) in the FA synthesis pathway. (**A**, **B**) Rapamycin titers in strains with the EQCi or *ermEp**-driving CRISPRi circuits harboring sgRNA targeting three *fabH* genes (*fabH1-H3*, encoding the 3-oxoacyl-ACP synthases). For the construction of EQCi or *ermEp**-driving CRISPRi circuits, one sgRNA (sg) was designed for each gene. Strains carrying the corresponding EQCi circuits were indicated by 2001/*sg-fabH1*, 2001/*sg-fabH2*, and 2001/*sg-fabH3*. Strains carrying the corresponding *ermEp**-driving CRISPRi circuits were indicated by 2001/*ermEp*/sg-fabH1*, 2001/*ermEp*/sg-fabH2*, and 2001/*ermEp*/sg-fabH3*. Samples were harvested from *S. rapamycinicus* strains grown in fermentation medium for 5, 7, 9, 11 and 13 days, respectively. The parental strain 2001 and 2001 carrying pSET-*srbAp-dcas9* (2001/*srbAp-dcas9*) or 2001 carrying pSET-*ermEp*-dcas9* (2001/*ermEp*-dcas9*) were used as controls. (**C**, **D**) Growth curves of *S. rapamycinicus* strains harboring the EQCi or *ermEp**-driving CRISPRi circuits targeting *fabH1-H3*. Samples were harvested from fermentation medium at the time points as indicated and the interval time is 12 h. Strans 2001 and 2001/*srbAp-dcas9* or 2001/*ermEp*-dcas9* were used as controls. (**E**, **F**) Transcriptional analysis of *fabH1-H3* in strains harboring the corresponding EQCi or *ermEp**-driving CRISPRi circuits by RT-qPCR. RNA samples were isolated from *S. rapamycinicus* strains grown in fermentation medium for 3, 5, 7 and 9 days, respectively. The relative transcript levels of each tested gene were normalized to *hrdB* (*M271_14880*, an internal control). The relative fold changes of gene transcription (the tested strains versus 2001/*srbAp-dcas9* or 2001/*ermEp*-dcas9*) were determined by the $2^{-\Delta\Delta CT}$ method. Error bars in (A–F) represent the standard deviations (SD) from three biological replicates.

node in the FA pathway resulted in growth arrest at very early stages, thereby leading to low biomass accumulation and suboptimal rapamycin titers. However, the EQCi circuits for dynamic repression were switched on during relatively late growth stages, resulting in build-up of sufficiently large biomass and accumulation of high rapamycin titers. Collectively, we successfully developed a novel pathway-independent dynamic regulation circuit (EQCi) for the repression of the key node in the FA pathway, which achieved a balance between bacterial growth and rapamycin biosynthesis, thereby resulting in significantly elevated rapamycin titers in *S. rapamycinicus*.

EQCi-mediated regulation of the TCA cycle

Two precursors for rapamycin biosynthesis, namely, malonyl-CoA and methylmalonyl-CoA (32), are mainly derived from acetyl-CoA. The TCA cycle, which is essential for cell growth, consumes a large number of acetyl-CoA molecules. We aimed to apply the EQCi circuit to dynamically inhibit the TCA cycle and divert acetyl-CoA flux towards malonyl-CoA and methylmalonyl-CoA biosynthesis to improve rapamycin production. The citric acid synthase catalyzes the formation of citric acid from acetyl-CoA and oxaloacetic acid, which is the first step of the TCA cycle involved in regulating the consumption of acetyl-CoA. Three genes (*M271_28125*, *M271_31465* and *M271_34825*) in *S. rapamycinicus* were predicted to encode citrate synthases (KEGG, https://www.kegg.jp/) and are named as *gltA*, *gltA1* and *gltA2*, respectively. They were selected for EQCi-mediated regulation. The sgRNAs of *gltA*, *gltA1*, and *gltA2* were designed to target nt 137–156 (*sg-gltA*), nt 8–27 (*sg-gltA1*), and nt 197–216 (*sg-gltA2*) with respect to the start codons, respectively. Six CRISPRi plasmids (Supplementary Table S1), including three EQCi plasmids (pSET-*srbAp-dcas9*/*sg-gltA*,

pSET-*srbAp-dcas9/sg-gltA1* and pSET-*srbAp-dcas9/sg-gltA2*) and three *ermEp**-driving CRISPRi plasmids (pSET-*ermEp*-dcas9/sg-gltA*, pSET-*ermEp*-dcas9/sg-gltA1* and pSET-*ermEp*-dcas9/sg-gltA2*) were constructed and introduced into *S. rapamycinicus*. We showed that EQCi-mediated silencing of the three respective *gltA* genes resulted in significantly enhanced rapamycin titers. The maximum titers of these engineered strains reached approximately 544 ± 66 mg/l (*gltA*), 471 ± 23 mg/l (*gltA1*) and 589 ± 46 mg/l (*gltA2*), which were approximately 125%, 95% and 143% higher, respectively, than those of the two control strains (Figure 3A). However, these three strains containing the corresponding *ermEp**-driving CRISPRi circuits produced drastically lower rapamycin titers than those of the controls (Figure 3B). Compared to the static regulation circuits, which resulted in drastically decreased biomass accumulation (Figure 3D), EQCi-based individual repression of the three *gltA* genes had little or no effect on cell growth (Figure 3C). We additionally showed that compared to highly reduced transcription of *gltA*, *gltA1* and *gltA2* in strains with static regulation circuits throughout the tested time course (3, 5, 7 and 9 days), the EQCi circuits resulted in gene downregulation in a cell density-dependent manner (Figure 3E and F) similar to that detected during dynamic regulation of the three *fabH* genes. Additionally, introduction of the control plasmids (pSET-*srbAp-dcas9* and pSET-*ermEp*-dcas9*) into 2001 had little effect on the transcription of *gltA-A2* (Supplementary Figure S4). The results clearly indicated that the EQCi circuits can achieve coordination of metabolic fluxes between the TCA cycle and rapamycin biosynthesis, thereby significantly elevating rapamycin titers.

EQCi-mediated downregulation of the AAA synthesis pathway

DHCHC is the starter unit of the rapamycin synthesis pathway (32,46). It is derived from the hydrolysis of chorismate which is naturally required for the synthesis of AAA, including phenylalanine (Phe), tyrosine (Tyr) and tryptophan (Trp). We applied the EQCi circuits to dynamically inhibit chorismate flux toward the biosynthesis of AAA, thereby increasing rapamycin titers. The reaction involved in the consumption of chorismate in the Phe and Tyr biosynthetic pathway is catalyzed by the chorismate mutase (CM), which is predicted to be encoded by four genes, including *M271_28280* (*cm1*), *M271_36305* (*cm2*), *M271_37500* (*cm3*) and *M271_43345* (*cm4*) (https://www.kegg.jp/). These four genes were selected for dynamic control. Four sgRNAs were designed to target nt 32–51 (*sg-cm1*), nt 149–168 (*sg-cm2*), nt 51–70 (*sg-cm3*) and nt 22–41 (*sg-cm4*), respectively. Accordingly, four EQCi plasmids (pSET-*srbAp-dcas9/sg-cm1*, pSET-*srbAp-dcas9/sg-cm2*, pSET-*srbAp-dcas9/sg-cm3* and pSET-*srbAp-dcas9/sg-cm4*) were constructed (Supplementary Table S1). As controls, four *ermEp**-driving CRISPRi plasmids (pSET-*ermEp*-dcas9/sg-cm1*, pSET-*ermEp*-dcas9/sg-cm2*, pSET-*ermEp*-dcas9/sg-cm3* and pSET-*ermEp*-dcas9/sg-cm4*) were also generated (Supplementary Table S1). These eight plasmids were individually introduced into *S. rapamycinicus* 2001. All four EQCi circuits caused significant elevation of rapamycin titers. The maximum titers of the four engineered strains reached approximately 316 ± 14 mg/l (*cm1*), 735 ± 52 mg/l (*cm2*), 693 ± 84 mg/l (*cm3*) and 694±31 mg/l (*cm4*), respectively (Figure 4A). However, the four strains carrying static regulation circuits produced drastically lower rapamycin titers than those of the controls (Figure 4B). We showed that when the EQCi circuits were employed, except for the strain carrying the EQCi circuit pSET-*srbAp-dcas9/sg-cm1* (repressing *cm1* expression) which exhibited slight growth arrest, the other three strains showed little or no growth changes compared to those of the controls (Figure 4C). However, static downregulation of these four genes resulted in much lower biomass accumulation (Figure 4D). We further confirmed that the transcript levels of these four target genes in strains containing the EQCi circuits were downregulated in a cell density-dependent manner as was described for dynamic regulation of the *fabH* and *gltA* genes, whereas gene transcription was constitutively repressed by static regulation circuits (Figure 4E and F). Notably, *cm1* transcription was the most significantly repressed, which may account for the growth arrest and lower rapamycin titers of the engineered strain carrying the EQCi plasmid pSET-*srbAp-dcas9/sg-cm1*. Similarly, introduction of the control plasmids (pSET-*srbAp-dcas9* and pSET-*ermEp*-dcas9*) into 2001 had little effect on the transcription of *cm1–4* (Supplementary Figure S5).

Combinatorial optimization of metabolic networks to substantially increase rapamycin production

As described above, dynamic downregulation of the three key nodes of the essential pathways, namely, the TCA cycle, FA synthesis pathway, and AAA synthesis pathway, achieved significantly enhanced rapamycin titers, respectively. With respect to each key node, which involves three or four predicted genes, dynamic regulation of *fabH3*, *cm2* and *gltA2* improved rapamycin production most significantly. We attempted to further increase rapamycin titers by performing dynamic downregulation of these three genes simultaneously using EQCi circuits. To this end, an EQCi circuit with three sgRNAs targeting *fabH3* (*sg-fabH3*), *gltA2* (*sg-gltA2*) and *cm2* (*sg-cm2*) was constructed and introduced into *S. rapamycinicus*. However, compared to the controls (2001 and 2001/*srbAp-dcas9*), the engineered strain 2002 carrying the EQCi circuit targeting three genes simultaneously showed severe growth arrest and decreased rapamycin titers in a cell density-dependent manner (Figure 5). When the cell density was relatively low (after three or four days of growth), cell growth and rapamycin titers of the engineered strain 2002 were comparable to those of the controls. However, strain 2002 subsequently accumulated much lower biomass and rapamycin titers than the controls. This finding clearly suggested that simultaneous silencing of these three target genes at their current regulation strengths may divert too much metabolic flux from these three pathways, resulting in an insufficient supply of metabolites for primary metabolism and leading to growth arrest and lower rapamycin biosynthesis. To exclude the possibility that the phenotypic alterations in 2002 occurred because of off-target effects of these three sgRNAs, we predicted the po-

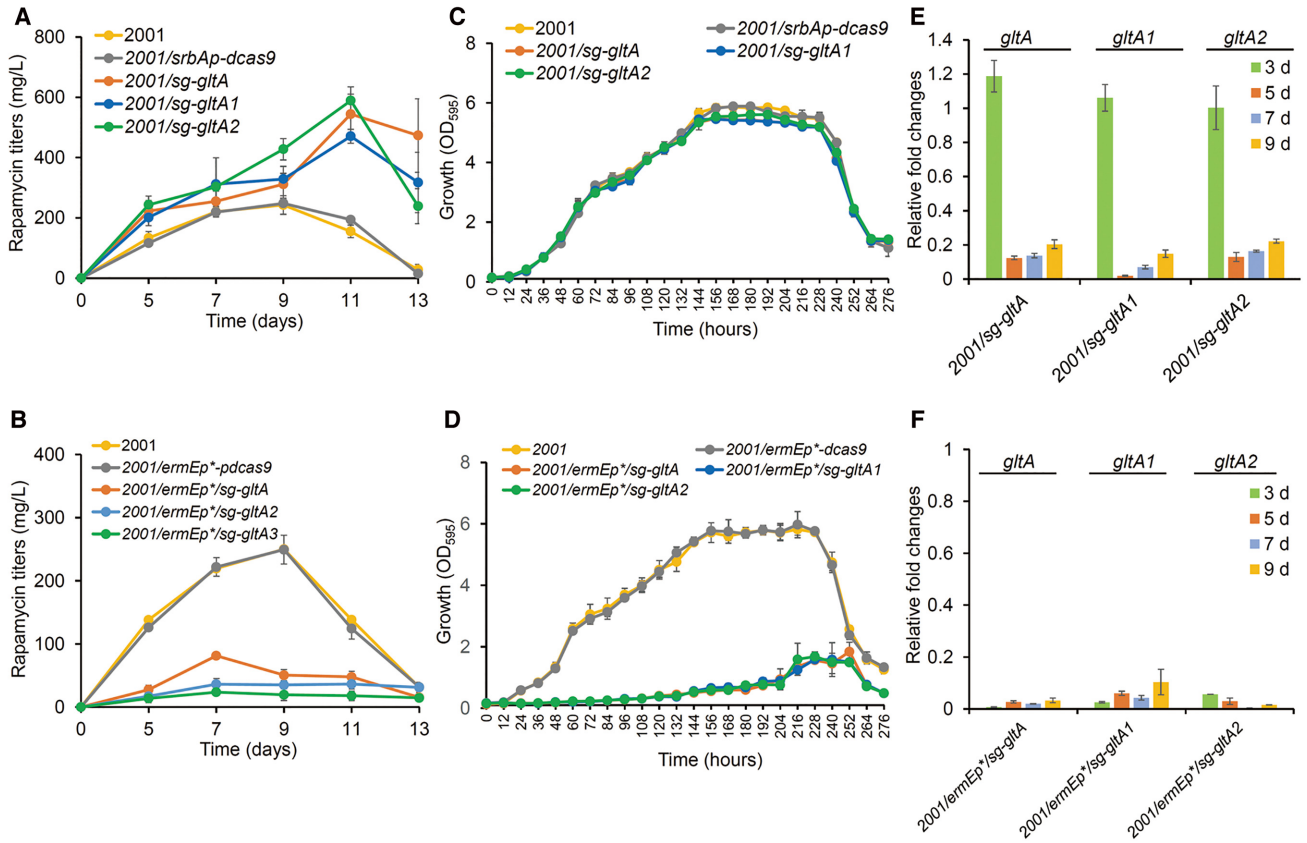

Figure 3. Effects of EQCi-mediated downregulation of the key node (citrate synthase) in the TCA cycle. (**A**, **B**) Rapamycin titers in strains with the EQCi or *ermEp**-driving CRISPRi circuits harboring sgRNA targeting three *gltA* genes (*gltA-A2*, encoding the citrate synthases). For the construction of EQCi or *ermEp**-driving CRISPRi circuits, one sgRNA (sg) was designed for each gene. Strains carrying the corresponding EQCi circuits were indicated by 2001/*sg-gltA*, 2001/*sg-gltA1*, and 2001/*sg-gltA2*. Strains carrying the corresponding *ermEp**-driving CRISPRi circuits were indicated by 2001/*ermEp*/sg-gltA*, 2001/*ermEp*/sg-gltA1*, and 2001/*ermEp*/sg-gltA2*. Samples were harvested from *S. rapamycinicus* strains grown in fermentation medium for 5, 7, 9, 11 and 13 days, respectively. Strains 2001 and 2001/*srbAp-dcas9* or 2001/*ermEp*-dcas9* were used as controls. The engineered strains in panel A were fermented together with those strains with the EQCi circuits targeting the *fabH* genes in Figure 2A. Therefore, the same rapamycin titers of the control strains (2001 and 2001/*srbAp-dcas9*) were used as those in Figure 2A. (**C**, **D**) Growth curves of *S. rapamycinicus* strains harboring the EQCi or *ermEp**-driving CRISPRi circuits targeting *gltA-A2*. Samples were harvested from fermentation medium at the time points as indicated and the interval time is 12 h. Strains 2001 and 2001/*srbAp-dcas9* or 2001/*ermEp*-dcas9* were used as controls. The engineered strains in panel C and D were fermented together with strains in Figure 2C and Figure 2D, respectively. Therefore, the same growth data of the control strains were used as those in Figure 2C (2001 and 2001/*srbAp-dcas9*) and 2D (2001 and 2001/*ermEp*-dcas9*). (**E**, **F**) Transcriptional analysis of *gltA-A2* in strains harboring the corresponding EQCi or *ermEp**-driving CRISPRi circuits by RT-qPCR. RNA samples were isolated from *S. rapamycinicus* strains grown in fermentation medium for 3, 5, 7 and 9 days, respectively. The relative transcript levels of each tested gene were normalized to *hrdB* (*M271_14880*, an internal control). The relative fold changes of gene transcription (the tested strains versus 2001/*srbAp-dcas9* or 2001/*ermEp*-dcas9*) were determined by the $2^{-\Delta\Delta CT}$ method. Error bars in (A–F) represent the standard deviations (SD) from three biological replicates.

tential off-targets of each sgRNA throughout the genome by CRISPy (36) (Supplementary Table S3). Then, the effects of three EQCi circuits harboring each sgRNA on the transcription of their corresponding off-targets were analyzed. Transcriptional analysis revealed only slightly reduced expression of two off-targets of *sg-cm2* (OT3 and OT4) in strain 2002 compared to the control strain 2001/*srbAp-dcas9* (Supplementary Figure S6). The results confirmed that growth arrest and lower rapamycin titers of 2002 occurred because of simultaneous repression of *fabH3*, *gltA2* and *cm2* at current repression strengths.

To search for a proper sgRNA combination with desired regulation strength, we created a library of EQCi circuits by changing the combination of three sgRNAs targeting *fabH3*, *gltA2* and *cm2* with different repression strengths. As a first step, we designed three additional sgRNAs for both *fabH3* and *gltA2*, and two additional sgRNAs for *cm2* (Figure 6A), attempted to obtain a series of sgRNAs with different regulation strengths. The corresponding EQCi circuits were constructed and introduced in *S. rapamycinicus* 2001. Next, three or four engineered strains containing different EQCi circuits for the dynamic downregulation of each gene were compared for cell growth, rapamycin titers, and gene transcription. For each tested gene, different effects were obtained by varying the targeting positions of sgRNAs (Figure 6 and Supplementary Figure S7). For dynamic regulation of *fabH3* and *cm2*, *sg-fabH3* and *sg-cm2* achieved the highest rapamycin titers (Figure 6B and D). For *gltA2*, *sg2-gltA2* resulted in the maximum rapamycin titer of 676±35 mg/l, which was approximately 27% higher than that of *sg-gltA2* (Figure 6C). Transcription analysis confirmed that EQCi-mediated repression is closely asso-

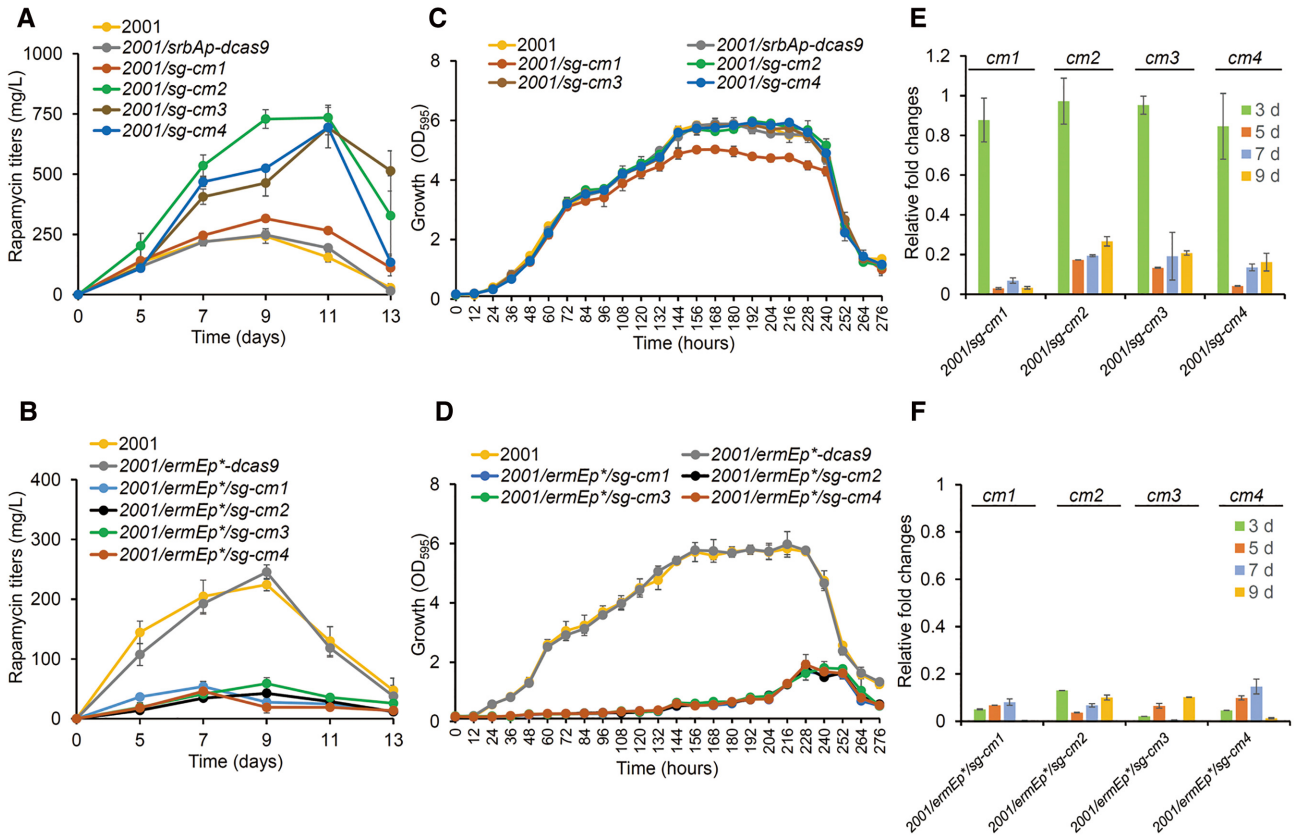

Figure 4. Effects of EQCi-mediated repression of the key node (chorismate mutase) in the AAA synthesis pathway. (**A**, **B**) Rapamycin titers in strains with the EQCi or *ermEp**-driving CRISPRi circuits harboring sgRNA targeting four *cm* genes (*cm1–4*, encoding the chorismate mutases). For the construction of the EQCi or *ermEp**-driving CRISPRi circuits, one sgRNA (sg) was designed for each gene. Strains carrying the corresponding EQCi circuits were indicated by 2001/*sg-cm1*, 2001/*sg-cm2*, 2001/*sg-cm3* and 2001/*sg-cm4*. Strains carrying the corresponding *ermEp**-driving CRISPRi circuits were indicated by 2001/*ermEp**/*sg-cm1*, 2001/*ermEp**/*sg-cm2*, 2001/*ermEp**/*sg-cm3* and 2001/*ermEp**/*sg-cm4*. Samples were harvested from *S. rapamycinicus* strains grown in fermentation medium for 5, 7, 9, 11 and 13 days, respectively. Strains 2001 and 2001/*srbAp-dcas9* or 2001/*ermEp*-dcas9* were used as controls. The engineered strains in panel A were fermented together with strains in Figures 2A and 3A. Therefore, the same rapamycin titers of the control strains (2001 and 2001/*srbAp-dcas9*) were used as those in Figures 2A and 3A. (**C**, **D**) Growth curves of *S. rapamycinicus* strains harboring the EQCi or *ermEp**-driving CRISPRi circuits targeting *cm1–4*. Samples were harvested from fermentation medium at the time points as indicated and the interval time is 12 h. Strains 2001 and 2001/*srbAp-dcas9* or 2001/*ermEp*-dcas9* were used as controls. The engineered strains in panel C and D were fermented together with strains in Figure 2C/3C and Figure 2D/3D, respectively. Therefore, the same growth data of the control strains were used as those in Figure 2C/3C (2001 and 2001/*srbAp-dcas9*) and Figure 2D/3D (2001 and 2001/*ermEp*-dcas9*). (**E**, **F**) Transcriptional analysis of *cm1–4* in strains harboring the corresponding EQCi or *ermEp**-driving CRISPRi circuits by RT-qPCR. RNA samples were isolated from *S. rapamycinicus* strains grown in fermentation medium for 3, 5, 7 and 9 days, respectively. The relative transcript levels of each tested gene were normalized to *hrdB* (*M271_14880*, an internal control). The relative fold changes of gene transcription (the tested strains versus 2001/*srbAp-dcas9* or 2001/*ermEp*-dcas9*) were determined by the $2^{-\Delta\Delta CT}$ method. Error bars in (A–F) represent the standard deviations (SD) from three biological replicates.

ciated with the targeting positions of sgRNA (Supplementary Figure S7). The closer the sgRNA targeting positions are to the start codons of target genes, the stronger the inhibition effect could be obtained. The growth curve further showed that EQCi circuits harboring the last three sgRNAs for *fabH3* and *gltA2*, or the last two sgRNAs for *cm2*, had little effect on bacterial growth (Supplementary Figure S7), suggesting that a trade-off was achieved between bacterial growth and product synthesis. Notably, compared to *sg-gltA2*, which caused drastic downregulation of *gltA2* transcription and evidently lower biomass accumulation, *sg2-gltA2* exerted little effect on cell growth and repressed gene transcription to a lesser extent (Supplementary Figure S7B and S7E), suggesting a more balanced state between the TCA cycle and rapamycin biosynthesis. In addition, EQCi circuits containing sgRNAs targeting too close to the start codon, including *sg1-fabH3*, *sg1-gltA2* and *sg1-cm2*, resulted in impaired cell growth, decreased rapamycin titers, and drastic gene downregulation in a cell density-dependent manner. The growth arrest and very low rapamycin titers of these three engineered strains were clearly associated with the drastic downregulation of the target genes after the cell density reached a threshold.

Given that *sg1-fabH3*, *sg1-gltA2* and *sg1-cm1* caused severe growth arrest, they were not considered for the purpose of library construction. Therefore, 18 EQCi circuits, each with a combination of three different sgRNAs (three sgRNAs for both *fabH3* and *gltA2*, two sgRNAs for *cm1*, $3 \times 3 \times 2 = 18$) were constructed and introduced into *S. rapamycinicus* 2001 (Figure 7A). We showed that among the 18 engineered strains carrying the corresponding EQCi circuit, four strains (2012, 2013, 2016, 2019) produced

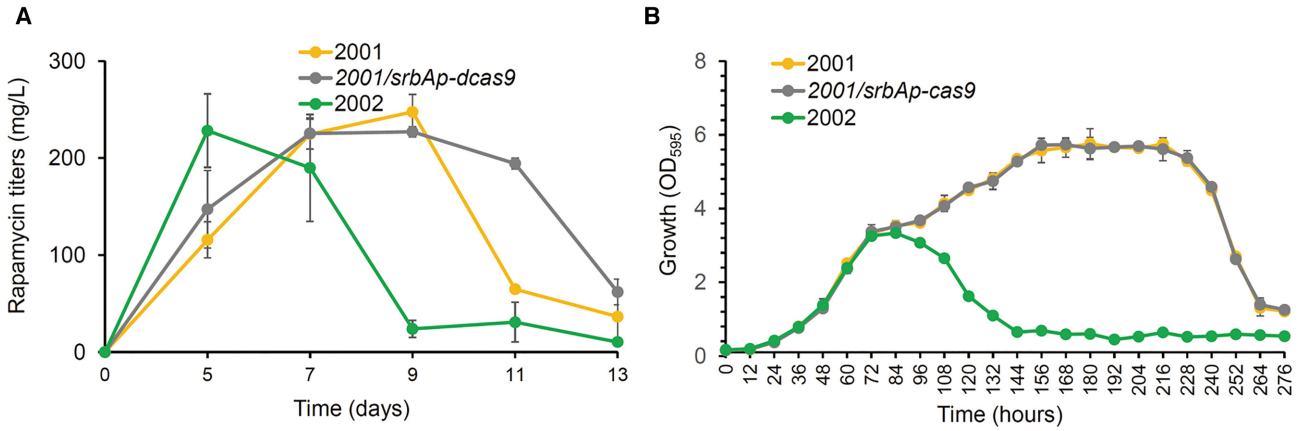

Figure 5. Effects of EQCi-mediated simultaneous downregulation of three key genes *fabH3*, *gltA2* and *cm2*. (**A**) Rapamycin titers in the strain with EQCi-mediated simultaneous repression of *fabH3*, *gltA2* and *cm2*. The strain with simultaneous dynamic repression of *fabH3*, *gltA2* and *cm2* was indicated by 2002 (containing the EQCi plasmid, pSET-*srbAp-dcas9-sg-fabH3//sg-gltA2/sg-cm2*). Samples were harvested from *S. rapamycinicus* strains grown in fermentation medium for 5, 7, 9, 11 and 13 days, respectively. 2001 and 2001/*srbAp-dcas9* were used as controls. (**B**) Growth curve of strain 2002 with EQCi-mediated simultaneous repression of *fabH3*, *gltA2* and *cm2*. Samples were harvested from fermentation medium at the time points as indicated and the interval time is 12 h. 2001 and 2001/*srbAp-dcas9* were used as controls. Error bars (A, B) denote the standard deviations (SD) of three biological replicates.

maximum rapamycin titers of over 1000 mg/l, which was much higher than those of the controls (247 ± 18 mg/l of 2001 and 239 ± 35 mg/l of 2001/*srbAp-dcas9*) (Figure 7B). Among them, strain 2012 with the EQCi circuit harboring the sgRNA combination of *sg2-gltA/sg3-fabH3/sg-cm2* showed the highest rapamycin titer of 1836±191 mg/l, which was ∼660% higher than those of the controls (Figure 7B). Next, we evaluated the growth curves and the target gene transcription of the top three high-yield rapamycin-producing strains (2012, 2013 and 2019). Little or no difference in cell growth was observed between the engineered strains and the controls (Figure 8A). It was further confirmed that target genes were dynamically regulated in a cell density-dependent manner. Because the sgRNA targeting positions that were located away from the start codons, the three target genes were repressed to a lesser extent from day 5 and transcript levels were downregulated to ∼27–57% of those of the control (Figure 8B–D). We found that the degree of transcription repression in the multiplexed EQCi environment was nearly the same as that in the CRISPRi-mediated single target environment. These data clearly suggest that EQCi-mediated repression of these three key genes at the proper repression strength, with particular reference to the sgRNA combination of *sg2-fabH3/sg3-gltA2/sg-cm2*, balanced metabolic fluxes between growth and rapamycin production.

DISCUSSION

In the current study, we designed and developed a novel pathway-independent dynamic control strategy, EQCi, in the important industrial strain, *S. rapamycinicus*, by integrating an endogenous QS system with the robust CRISPRi tool. The EQCi genetic circuit was successfully applied to implement fully autonomous, tunable, and dynamic downregulation of three key nodes in essential pathways, either separately or simultaneously, to divert metabolic fluxes towards rapamycin biosynthesis in a cell population density-dependent manner, thereby achieving substantial increases in rapamycin titers. Remarkably, the EQCi-mediated multiplexed control of essential pathways at proper repression strengths imposed little or no metabolic burden on cell growth, which indicated its ability to effectively coordinate the distribution of metabolic fluxes between cell growth and rapamycin biosynthesis. Pathway-independent QS circuits was previously shown to be effective for improving the titers of target products (18–22). However, in bacteria, all previous pathway-independent QS circuits were built on heterologous systems. To ensure the effectiveness of QS-based dynamic circuits, repeated screening, and optimization of the *cis*-regulatory elements (including promoters and RBS) driving the expression of QS modules, involving the construction of promoter-RBS libraries, are generally required. This is both labor-intensive and time-consuming. Normally, to dynamically regulate one gene or an operon, three to five promoters and the same number (three to five) of different RBSs are required to screen for the appropriate switching time and desired regulation strength (19–21). Accordingly, 9–25 plasmids and strains need to be constructed. If two to three genes are regulated simultaneously with different regulation strengths, up to 9^2–25^2 and 9^3–25^3 plasmid constructs and strains need to be generated, which is challenging. Therefore, in previous studies, only one gene or an operon was regulated dynamically or two to three genes or operons were regulated together at the same regulation strength (19–21), limiting the development of strains with better performance. Our EQCi strategy is very convenient because it directly places dCas9 expression under the regulation of a QS signal (GBLs)-responsive promoter, which easily addresses the above stated challenges. The switching time for EQCi-mediated regulation is cell density-dependent and does not require optimization. Different regulation strengths in EQCi can be readily achieved by changing the sgRNA targeting positions. Thus, EQCi-based multiplex dynamic regulation is labor-and time-saving compared to the heterologous QS-mediated methods. Finally,

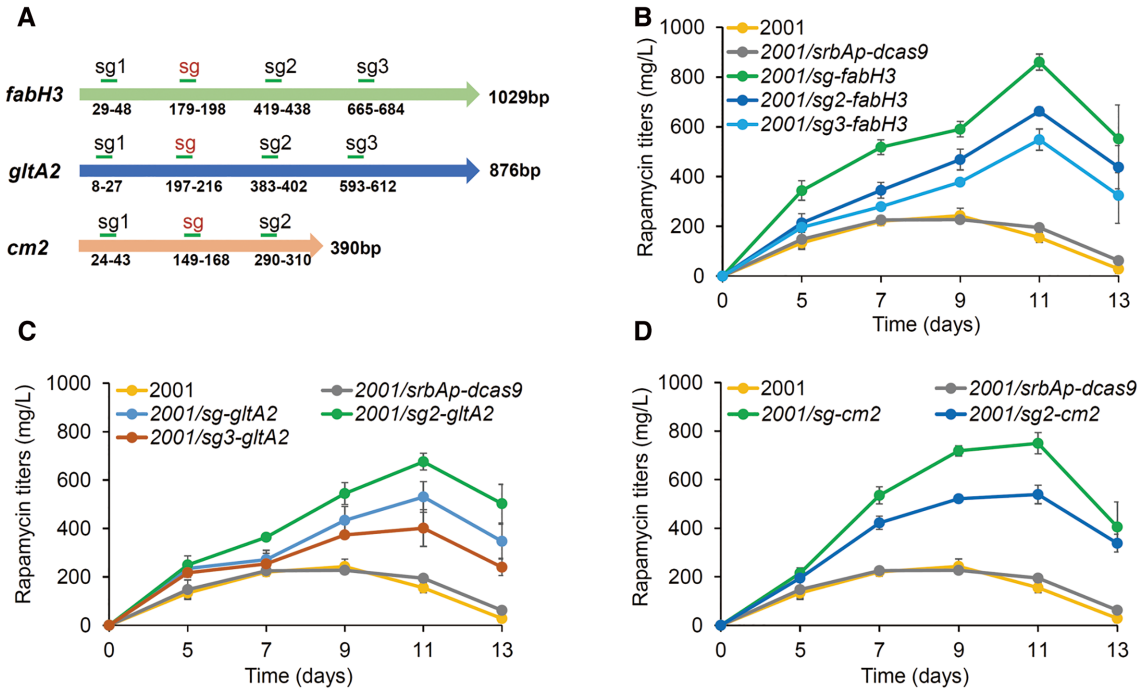

Figure 6. Effects of EQCi-mediated individual dynamic regulation of three key genes *fabH3*, *gltA2* and *cm2* on rapamycin titers by varying sgRNA targeting positions. (**A**) Schematic diagram of the sgRNA targeting positions designed on the non-template strands of the coding regions of *fabH3*, *gltA2* and *cm2*. The targeting positions are as indicated. sgRNAs that have been tested in the above experiments are presented by red font. (**B–D**) Rapamycin titers in strains with the EQCi circuits targeting *fabH3* (three designed sgRNAs), *gltA2* (three designed sgRNAs) and *cm2* (two designed sgRNAs), respectively. Strains with the corresponding EQCi circuits were as indicated. Samples were collected from *S. rapamycinicus* strains grown in fermentation medium for 5, 7, 9, 11 and 13 days, respectively. 2001 and 2001/*srbAp-dcas9* were used as controls. Error bars denote the standard deviations (SD) of three biological replicates. The engineered strains in panels B, C and D were fermented together. Therefore, the same growth data of the two control strains (2001 and 2001/*srbAp-dcas9*) were used.

the wide distribution of QS systems in microbes, as well as the simplicity and specificity of CRISPRi (28), indicates that the EQCi-mediated regulation strategy can be easily expanded to engineer other microbial cell factories.

To demonstrate the applicability of our EQCi system, we applied it in the model strain *S. coelicolor* which produces the blue-colored polyketide antibiotic actinorhodin (47). We constructed the EQCi plasmid, pSET-*scbAp-dcas9/sg-gltA(sco)* (Supplementary Table S1), in which the endogenous GBL-responsive promoter in *S. coelicolor*, *scbAp*, was used to drive dCas9 expression and the *j23119* promoter was used to regulate the transcription of sgRNA targeting the *gltA* gene (*sco2736*) in the TCA cycle. The strain carrying the above EQCi plasmid produced ~850% higher actinorhodin titers than the controls (Supplementary Figure S8). Overall, EQCi system-mediated dynamic regulation of essential pathways shows great potential to become a universal technology for strain improvements.

Prior to our study, static metabolic engineering has been employed to enhance rapamycin production. For example, chromosomal integration of an additional copy of two cluster-situated activator genes *rapG* and *rapH* resulted in 20–32% and 27–55% increases in rapamycin titers, respectively (48). In another study, based on a genome-scale metabolic model, *pfk* (encoding 6-phosphofructokinase) was deleted, and two target genes including *dahp* (encoding a DAHP synthase) and *rapK* (encoding a chorismatase) were overexpressed, resulting in approximately 30.8%, 36.2% and 44.8% increases in rapamycin titers, respectively. Combinatorial metabolic engineering by *pfk* knockout and co-overexpression of *dahP* and *rapK*, led to further enhanced rapamycin production by 142.3%, achieving a 250.8 mg/l rapamycin titer (49). Thus, compared to previous studies utilizing static metabolic engineering approaches, our EQCi-based regulation of multiple essential pathways is much more effective for improving rapamycin titers.

The rapamycin titers of *S. rapamycinicus*, particularly high-yield engineered strains, decreased sharply in the late fermentation stages (on day 11) (Figure 2–6). Similar phenomena were reported previously (50,51) and are likely to be ascribed to rapamycin degradation (51). The detailed mechanism for this phenomenon remains elusive. In addition, we observed a drastic reduction in the cell growth of *S. rapamycinicus* strains after fermentation for 10 days. This may be resulted from nutrition depletion in the late stage of fermentation. Meanwhile, acid fermentation condition (approximately pH 4.5) after growth for 10 days may also be involved.

Rapamycin, as a complex natural product of polyketide, provides a good example for EQCi system-mediated titer improvements of other polyketide compounds. Polyketide biosynthesis requires a variety of common precursors, such as malonyl-CoA, methymalonyl-CoA, and isobutyryl-CoA, which are mainly derived from acetyl-CoA. Therefore, the two essential pathways tested, including the TCA cycle and FA synthesis pathway, can be used as universal targets for EQCi regulation to increase polyketide titers. In

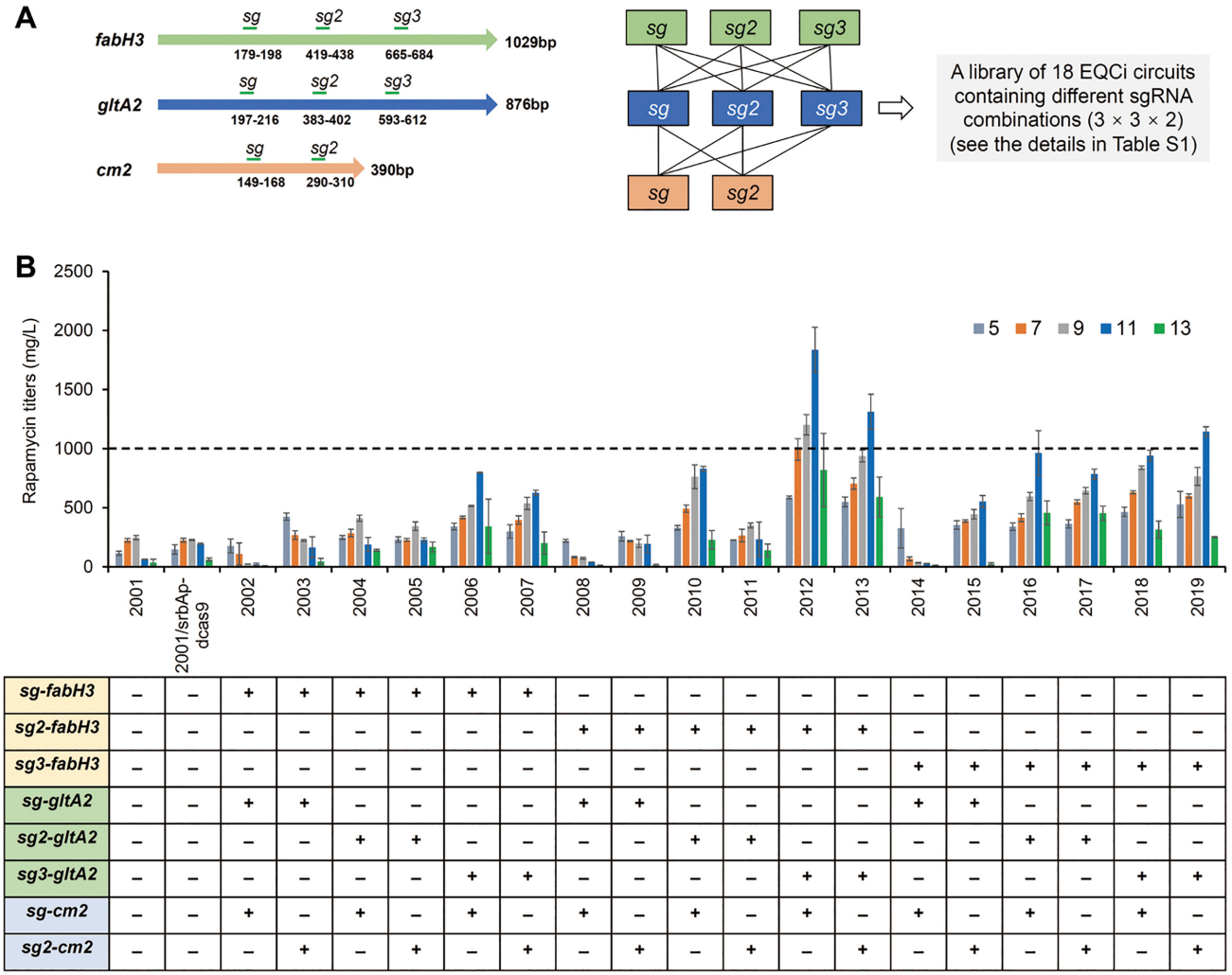

Figure 7. Design of a library of the EQCi genetic circuits with different sgRNA combinations (**A**) and rapamycin titers in strains with EQCi-mediated simultaneous repression of *fabH3, gltA2* and *cm2* with varying repression strengths (**B**). The combinations of three different gRNAs were presented below the strains as indicated (from 2002 to 2019). Samples for analyzing rapamycin titers were collected from *S. rapamycinicus* strains grown in fermentation medium for 5, 7, 9, 11 and 13 days, respectively. 2001 and 2001/*srbAp-dcas9* were used as controls. Error bars denote the standard deviations (SD) of three biological replicates.

future research, other essential pathways such as glycolysis and the pentose phosphate pathway may be included as well for EQCi regulation to globally optimize the metabolic networks, which may achieve better titer improvements. Nevertheless, testing and screening of key nodes in these primary pathways and optimization of gene repression strengths may be required for different target products.

Each key node we selected for dynamic regulation, was represented by three or four encoding genes (isozyme genes). This information was obtained from the KEGG database (https://www.kegg.jp/). At present, their specific functions remain unidentified. Based on the growth arrest phenotypes resulting from static gene regulation, we confirmed that these genes were required for normal cell growth and that none were redundant in *S. rapamycinicus*. EQCi-mediated repression of these genes resulted in an obvious increase in rapamycin production. To determine the effect of combinatorial repression of the three essential pathways, we selected only one gene from each node, the dynamic regulation of which resulted in the most significantly enhanced rapamycin production. Screening a library of 18 engineered strains harboring different sgRNA combinations enabled us to obtain the strain with a final rapamycin titer of 1836 ± 191 mg/l. Thus, designing more sgRNAs for each gene and including more isozyme genes may enable strains with higher rapamycin titers to be obtained by screening of a larger library via high-throughput screening technology.

EQCi circuits incorporate advantages associated with both the QS system and CRISPRi, enabling tunable, fully autonomous, and dynamic downregulation of single or multiple pathways leading to the redirection of metabolic fluxes, thereby maximizing target product biosynthesis without human intervention. However, dual-regulation genetic circuits which restrict metabolic flux through primary metabolism and siphon it into the rapamycin biosynthesis pathway simultaneously were not evaluated. Combined with the results obtained for EQCi-mediated repression, implementing dynamic upregulation to improve the expression of key nodes in the rapamycin biosynthetic pathway may further enhance its titers.

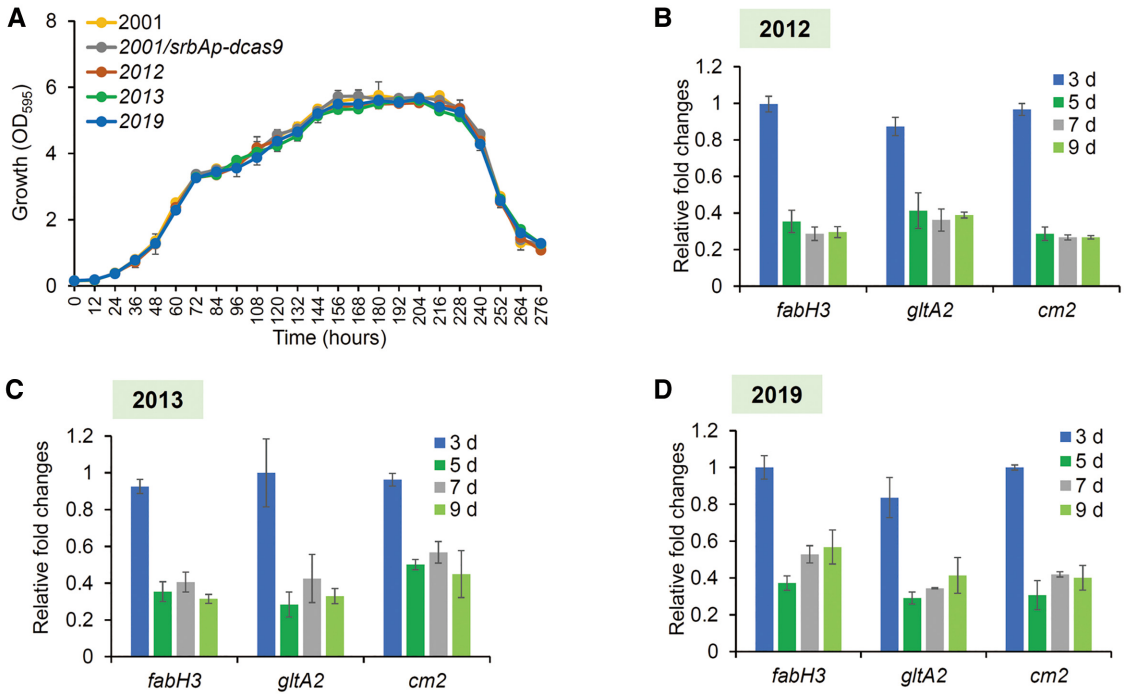

Figure 8. Effects of the EQCi circuits for simultaneous downregulation of three key genes *fabH3*, *gltA2* and *cm2* with proper repression strength on cell growth and gene transcription. (**A**) Growth curves of the top three high-yield rapamycin-producing strains harboring EQCi circuit-mediated simultaneous repression of *fabH3, gltA2* and *cm2* with proper repression strength. The three strains were indicated as 2012 (harboring the EQCi plasmid pSET-*srbAp-dcas9-sg2-fabH3/sg3-gltA2/sg-cm2*), 2013 (harboring the EQCi plasmid pSET-*srbAp-dcas9-sg2-fabH3/sg3-gltA2/sg2-cm2*) and 2019 (harboring the EQCi plasmid, pSET-*srbAp-dcas9-sg3-fabH3/sg3-gltA2/sg2-cm2*), respectively. Samples were collected from *S. rapamycinicus* strains grown in fermentation medium for 5, 7, 9, 11 and 13 days. 2001 and 2001/*srbAp-dcas9* were used as controls. (**B–D**) Transcript levels of *fabH3, gltA2* and *cm2* in the top three high-yield rapamycin-producing strains (2012, 2013 and 2019). RNA samples were isolated from *S. rapamycinicus* strains grown in fermentation medium for 3, 5, 7 and 9 days, respectively. The relative transcript levels of each tested gene were normalized to *hrdB* (*M271_14880*, an internal control). The relative fold changes of gene transcription (the tested strains versus 2001/*srbAp-dcas9*) were determined by the $2^{-\Delta\Delta CT}$ method. Error bars in (A–D) represent the standard deviations (SD) from three biological replicates.

SUPPLEMENTARY DATA

Supplementary Data are available at NAR Online.

ACKNOWLEDGEMENTS

Author contributions: J.T. and G.Y. performed experiments and drafted the manuscript. X.S. provided the parental strain of *S. rapamycinicus* and medium formula for bacterial fermentations. Y.G. contributed the editing of the manuscript. Y.L. and W.J. designed research, analyzed data and contributed to the writing and editing of the manuscript.

FUNDING

National Key Research and Development Program [2019YFA0905400 to Y.L., 2018YFA0903700 to G.Z.]; National Natural Science Foundation of China [31770088 to Y.L., 31921006 to W.J.]; National Mega-project for Innovative Drugs [2018ZX09711001-006-012 to Y.L.]. Funding for open access charge: National Natural Science Foundation of China.
Conflict of interest statement. None declared.

REFERENCES

1. Cress,B.F., Trantas,E.A., Ververidis,F., Linhardt,R.J. and Koffas,M.A. (2015) Sensitive cells: enabling tools for static and dynamic control of microbial metabolic pathways. *Curr. Opin. Biotechnol.*, **36**, 205–214.
2. Li,L., Zhao,Y., Ruan,L., Yang,S., Ge,M., Jiang,W. and Lu,Y. (2015) A stepwise increase in pristinamycin II biosynthesis by *Streptomyces pristinaespiralis* through combinatorial metabolic engineering. *Metab. Eng.*, **29**, 12–25.
3. Solomon,K.V., Sanders,T.M. and Prather,K.L. (2012) A dynamic metabolite valve for the control of central carbon metabolism. *Metab. Eng.*, **14**, 661–671.
4. Tan,S.Z., Manchester,S. and Prather,K.L. (2016) Controlling central carbon metabolism for improved pathway yields in *Saccharomyces cerevisiae*. *ACS Synth. Biol.*, **5**, 116–124.
5. Liang,C., Zhang,X., Wu,J., Mu,S., Wu,Z., Jin,J.M. and Tang,S.Y. (2020) Dynamic control of toxic natural product biosynthesis by an artificial regulatory circuit. *Metab. Eng.*, **57**, 239–246.
6. Shi,S., Ang,E.L. and Zhao,H. (2018) *In vivo* biosensors: mechanisms, development, and applications. *J. Ind. Microbiol. Biotechnol.*, **45**, 491–516.
7. Mahr,R. and Frunzke,J. (2016) Transcription factor-based biosensors in biotechnology: current state and future prospects. *Appl. Microbiol. Biotechnol.*, **100**, 79–90.
8. Brockman,I.M. and Prather,K.L. (2015) Dynamic metabolic engineering: new strategies for developing responsive cell factories. *Biotechnol. J.*, **10**, 1360–1369.
9. Liu,D., Mannan,A.A., Han,Y., Oyarzun,D.A. and Zhang,F. (2018) Dynamic metabolic control: towards precision engineering of metabolism. *J. Ind. Microbiol. Biotechnol.*, **45**, 535–543.

10. Shen,X., Wang,J., Li,C., Yuan,Q. and Yan,Y. (2019) Dynamic gene expression engineering as a tool in pathway engineering. *Curr. Opin. Biotechnol.*, **59**, 122–129.
11. Lalwani,M.A., Zhao,E.M. and Avalos,J.L. (2018) Current and future modalities of dynamic control in metabolic engineering. *Curr. Opin. Biotechnol.*, **52**, 56–65.
12. Liu,D., Evans,T. and Zhang,F. (2015) Applications and advances of metabolite biosensors for metabolic engineering. *Metab. Eng.*, **31**, 35–43.
13. Farmer,W.R. and Liao,J.C. (2000) Improving lycopene production in *Escherichia coli* by engineering metabolic control. *Nat. Biotechnol.*, **18**, 533–537.
14. Zhang,F., Carothers,J.M. and Keasling,J.D. (2012) Design of a dynamic sensor-regulator system for production of chemicals and fuels derived from fatty acids. *Nat. Biotechnol.*, **30**, 354–359.
15. Dahl,R.H., Zhang,F., Alonso-Gutierrez,J., Baidoo,E., Batth,T.S., Redding-Johanson,A.M., Petzold,C.J., Mukhopadhyay,A., Lee,T.S., Adams,P.D. *et al.* (2013) Engineering dynamic pathway regulation using stress-response promoters. *Nat. Biotechnol.*, **31**, 1039–1046.
16. Zhou,L.B. and Zeng,A.P. (2015) Engineering a lysine-ON riboswitch for metabolic control of lysine production in *Corynebacterium glutamicum*. *ACS Synth. Biol.*, **4**, 1335–1340.
17. Wu,Y., Chen,T., Liu,Y., Tian,R., Lv,X., Li,J., Du,G., Chen,J., Ledesma-Amaro,R. and Liu,L. (2020) Design of a programmable biosensor-CRISPRi genetic circuits for dynamic and autonomous dual-control of metabolic flux in *Bacillus subtilis*. *Nucleic. Acids. Res.*, **48**, 996–1009.
18. Williams,T.C., Averesch,N.J.H., Winter,G., Plan,M.R., Vickers,C.E., Nielsen,L.K. and Kromer,J.O. (2015) Quorum-sensing linked RNA interference for dynamic metabolic pathway control in *Saccharomyces cerevisiae*. *Metab. Eng.*, **29**, 124–134.
19. Doong,S.J., Gupta,A. and Prather,K.L.J. (2018) Layered dynamic regulation for improving metabolic pathway productivity in *Escherichia coli*. *Proc. Natl. Acad. Sci. U.S.A.*, **115**, 2964–2969.
20. Dinh,C.V. and Prather,K.L.J. (2019) Development of an autonomous and bifunctional quorum-sensing circuit for metabolic flux control in engineered *Escherichia coli*. *Proc. Natl. Acad. Sci. U.S.A.*, **116**, 25562–25568.
21. Gupta,A., Reizman,I.M., Reisch,C.R. and Prather,K.L. (2017) Dynamic regulation of metabolic flux in engineered bacteria using a pathway-independent quorum-sensing circuit. *Nat. Biotechnol.*, **35**, 273–279.
22. Soma,Y. and Hanai,T. (2015) Self-induced metabolic state switching by a tunable cell density sensor for microbial isopropanol production. *Metab. Eng.*, **30**, 7–15.
23. Papenfort,K. and Bassler,B.L. (2016) Quorum sensing signal-response systems in Gram-negative bacteria. *Nat. Rev. Microbiol.*, **14**, 576–588.
24. Whiteley,M., Diggle,S.P. and Greenberg,E.P. (2017) Progress in and promise of bacterial quorum sensing research. *Nature*, **551**, 313–320.
25. Minogue,T.D., Wehland-von Trebra,M., Bernhard,F. and von Bodman,S.B. (2002) The autoregulatory role of EsaR, a quorum-sensing regulator in *Pantoea stewartii* ssp. stewartii: evidence for a repressor function. *Mol. Microbiol.*, **44**, 1625–1635.
26. Takano,E. (2006) Gamma-butyrolactones: *Streptomyces* signalling molecules regulating antibiotic production and differentiation. *Curr. Opin. Microbiol.*, **9**, 287–294.
27. Gilbert,L.A., Larson,M.H., Morsut,L., Liu,Z., Brar,G.A., Torres,S.E., Stern-Ginossar,N., Brandman,O., Whitehead,E.H., Doudna,J.A. *et al.* (2013) CRISPR-mediated modular RNA-guided regulation of transcription in eukaryotes. *Cell*, **154**, 442–451.
28. Qi,L.S., Larson,M.H., Gilbert,L.A., Doudna,J.A., Weissman,J.S., Arkin,A.P. and Lim,W.A. (2013) Repurposing CRISPR as an RNA-guided platform for sequence-specific control of gene expression. *Cell*, **152**, 1173–1183.
29. Jakociunas,T., Jensen,M.K. and Keasling,J.D. (2017) System-level perturbations of cell metabolism using CRISPR/Cas9. *Curr. Opin. Biotechnol.*, **46**, 134–140.
30. Tarasava,K., Oh,E.J., Eckert,C.A. and Gill,R.T. (2018) CRISPR-enabled tools for engineering microbial genomes and phenotypes. *Biotechnol. J.*, **13**, e1700586.
31. Fontana,J., Dong,C., Ham,J.Y., Zalatan,J.G. and Carothers,J.M. (2018) Regulated expression of sgRNAs tunes CRISPRi in *E. coli*. *Biotechnol. J.*, **13**, e1800069.
32. Yoo,Y.J., Kim,H., Park,S.R. and Yoon,Y.J. (2017) An overview of rapamycin: from discovery to future perspectives. *J. Ind. Microbiol. Biotechnol.*, **44**, 537–553.
33. Chung,C.L., Lawrence,I., Hoffman,M., Elgindi,D., Nadhan,K., Potnis,M., Jin,A., Sershon,C., Binnebose,R., Lorenzini,A. *et al.* (2019) Topical rapamycin reduces markers of senescence and aging in human skin: an exploratory, prospective, randomized trial. *Geroscience*, **41**, 861–869.
34. Tummala,S.B., Welker,N.E. and Papoutsakis,E.T. (1999) Development and characterization of a gene expression reporter system for *Clostridium acetobutylicum* ATCC 824. *Appl. Environ. Microbiol.*, **65**, 3793–3799.
35. Zhao,Y., Li,L., Zheng,G., Jiang,W., Deng,Z., Wang,Z. and Lu,Y. (2018) CRISPR/dCas9-mediated multiplex gene repression in *Streptomyces*. *Biotechnol. J.*, **13**, 1800121.
36. Blin,K., Pedersen,L.E., Weber,T. and Lee,S.Y. (2016) CRISPy-web: an online resource to design sgRNAs for CRISPR applications. *Synth. Syst. Biotechnol.*, **1**, 118–121.
37. Kieser,T., Bibb,M.J., Buttner,M.J. and Chater,K.F. (2000) In: *Practical Streptomyces Genetics*. John Innes Foundation, Norwich, England.
38. Zhao,Y., Xiang,S., Dai,X. and Yang,K. (2013) A simplified diphenylamine colorimetric method for growth quantification. *Appl. Microbiol. Biotechnol.*, **97**, 5069–5077.
39. Wang,R., Mast,Y., Wang,J., Zhang,W., Zhao,G., Wohlleben,W., Lu,Y. and Jiang,W. (2013) Identification of two-component system AfsQ1/Q2 regulon and its cross-regulation with GlnR in *Streptomyces coelicolor*. *Mol. Microbiol.*, **87**, 30–48.
40. Livak,K.J. and Schmittgen,T.D. (2001) Analysis of relative gene expression data using real-time quantitative PCR and the 2(-Delta Delta C(T)) Method. *Methods*, **25**, 402–408.
41. Horinouchi,S. (2002) A microbial hormone, A-factor, as a master switch for morphological differentiation and secondary metabolism in *Streptomyces griseus*. *Front. Biosci.*, **7**, d2045–2057.
42. Takano,E., Kinoshita,H., Mersinias,V., Bucca,G., Hotchkiss,G., Nihira,T., Smith,C.P., Bibb,M., Wohlleben,W. and Chater,K. (2005) A bacterial hormone (the SCB1) directly controls the expression of a pathway-specific regulatory gene in the cryptic type I polyketide biosynthetic gene cluster of *Streptomyces coelicolor*. *Mol. Microbiol.*, **56**, 465–479.
43. Mehra,S., Charaniya,S., Takano,E. and Hu,W.S. (2008) A bistable gene switch for antibiotic biosynthesis: the butyrolactone regulon in *Streptomyces coelicolor*. *PLoS One*, **3**, e2724.
44. He,H., Ye,L., Li,C., Wang,H., Guo,X., Wang,X., Zhang,Y. and Xiang,W. (2018) SbbR/SbbA, an important ArpA/AfsA-like system, regulates milbemycin production in *Streptomyces bingchenggensis*. *Front. Microbiol.*, **9**, 1064.
45. Biarnes-Carrera,M., Lee,C.K., Nihira,T., Breitling,R. and Takano,E. (2018) Orthogonal regulatory circuits for *Escherichia coli* based on the gamma-butyrolactone system of *Streptomyces coelicolor*. *ACS Synth. Biol.*, **7**, 1043–1055.
46. Andexer,J.N., Kendrew,S.G., Nur-e-Alam,M., Lazos,O., Foster,T.A., Zimmermann,A.S., Warneck,T.D., Suthar,D., Coates,N.J., Koehn,F.E. *et al.* (2011) Biosynthesis of the immunosuppressants FK506, FK520, and rapamycin involves a previously undescribed family of enzymes acting on chorismate. *Proc. Natl. Acad. Sci. U.S.A.*, **108**, 4776–4781.
47. Malpartida,F. and Hopwood,D.A. (1986) Physical and genetic characterisation of the gene cluster for the antibiotic actinorhodin in *Streptomyces coelicolor* A3(2). *Mol. Gen. Genet.*, **205**, 66–73.
48. Kuscer,E., Coates,N., Challis,I., Gregory,M., Wilkinson,B., Sheridan,R. and Petkovic,H. (2007) Roles of *rapH* and *rapG* in positive regulation of rapamycin biosynthesis in *Streptomyces hygroscopicus*. *J. Bacteriol.*, **189**, 4756–4763.
49. Dang,L., Liu,J., Wang,C., Liu,H. and Wen,J. (2017) Enhancement of rapamycin production by metabolic engineering in *Streptomyces hygroscopicus* based on genome-scale metabolic model. *J. Ind. Microbiol. Biotechnol.*, **44**, 259–270.
50. Xu,Z.N., Shen,W.H., Chen,X.Y., Lin,J.P. and Cen,P.L. (2005) A high-throughput method for screening of rapamycin-producing strains of *Streptomyces hygroscopicus* by cultivation in 96-well microtiter plates. *Biotechnol. Lett.*, **27**, 1135–1140.
51. Dutta,S., Basak,B., Bhunia,B., Chakraborty,S. and Dey,A. (2014) Kinetics of rapamycin production by *Streptomyces hygroscopicus* MTCC 4003. *3 Biotech.*, **4**, 523–531.